ISSN 2354-9114 (online), ISSN 0024-9521 (print)
Indonesian Journal of Geography Vol.52, No. 3, 2020 (402 – 410)
DOI: http://dx.doi.org/10.22146/ijg.53740 website: https://jurnal.ugm.ac.id/ijg

INDONESIAN JOURNAL OF GEOGRAPHY

RESEARCH ARTICLE

Topography and structural changes of Anak Krakatau due to the December 2018 catastrophic events

Herlan Darmawan[1*], Bachtiar W. Mutaqin[2], Wahyudi[1], Agung Harijoko[3], Haryo Edi Wibowo[3], Nia Haerani[4], Mamay Surmayadi[4], Syarifudin[5], Raditya Jati[6], Suratman[2] and Wikanti Asriningrum[7]

[1] Laboratory of Geophysics, Department of Physics, Faculty of Mathematics and Natural Sciences, Universitas Gadjah Mada, Sekip Utara, Bulaksumur, Yogyakarta, Indonesia
[2]Department of Environmental Geography, Faculty of Geography, Universitas Gadjah Mada, Sekip Utara, Bulaksumur, Indonesia
[3] Department of Geological Engineering, Faculty of Engineering, Universitas Gadjah Mada, Indonesia
[4] Center for Volcanology and Geological Hazards Mitigation, Geological Agency, Ministry of Energy and Mineral Resources, Bandung, Indonesia
[5] Bengkulu - Lampung Natural Resource Conservation Agency, Jl. Z.A. Pagar alam No. 1B Rajabasa Bandar Lampung
[6] Indonesian National Board for Disaster Management, Jl. Pramuka Kav. 38 Jakarta Timur 13120
[7] Remote sensing application center, National Institute of Aeronautics and Space of Indonesia, Pasar Rebo, Jakarta Timur, Indonesia

Received: 2020-04-11
Accepted: 2020-11-24

Keywords:
Anak Krakatau;
the 22 December flank collapse;
Digital Elevation Model;
Topography and structural changes

Correspondent email:
herlan_darmawan@mail.ugm.ac.id

Abstract. The flank collapse of Anak Krakatau on 22 December 2018 caused massive topography losses that generated a devastating tsunami in Sunda Strait, which then followed by eruptions that progressively changed the topography and structure of Anak Krakatau. Here, we investigated topography and structural changes due to the December 2018 flank collapse and the following eruptions by using high resolution Digital Elevation Model (DEM) before and after the events and sentinel 1A satellite image post-flank collapsed. Results show that the volumetric losses due to the 22 December 2018 flank collapsed is ~127 x 10^6 m^3, while the following eruptions caused ~0,8 x 10^6 m^3 losses. Structural investigation suggests two structures that may act as failure planes. The first structure is located at the western part of volcanic edifice that associated with hydrothermal alteration and the second failure is an old crater rim which delineated an actively deform volcanic cone.

1. Introduction

The flank collapse of an active volcano is one of the most catastrophic natural hazards on Earth as it may generate catastrophic debris flows that is destroyed within a large area. The 1980 flank collapse of Mt. St. Helens in US generated high energetic debris avalanche with total volume of 2.5 km^3 and maximum run out distance of 23 km (USGS, 2017). Moreover, the flank collapse may occur in an active submarine volcano that can trigger devastating tsunami, such as the 22 December 2018 flank collapse of Anak Krakatau that claimed 437 victims, ten people losses, and 31.943 injured (BNPB, 2019). This high number of casualties existed as the 22 December 2018 flank collapsed of Anak Krakatau occurred during holiday peak season in Sunda Strait. Even though this sector collapsed event has been investigated based on geomorphology of Anak Krakatau and numerical model of tsunami propagation (Giachetti, Paris, Kelfoun, & Ontowirjo, 2012), however, such event is challenging to forecast. Therefore, understanding the mechanism of flank collapsed of active submarine volcano that located close to densely populated area is vital for volcano risk management.

There are several mechanisms that can contribute toward the development of volcano flank failure, which structural instability is commonly found in this case. The development of weak core due to hydrothermal activity that causing edifice spreading and reducing the rock strength and friction (Mayer et al., 2016; Meller & Kohl, 2014), volcanic seismicity, and slope oversteepening can destabilize the structure (Mcguire, 1996). Moreover, an injection of new magma can increase pore fluid pressure beneath the volcanic edifice that can add forces and lead to failure (Famin & Michon, 2010).

Here, we investigate structural instability that may trigger the 22 December volcanic flank collapse of Anak Krakatau. We conducted high resolution topographic mapping by combining drone photogrammetry and bathymetry field campaigns after the December 2018 catastrophic events. Drone photogrammetry is robust to reconstruct complex terrain of active volcano with sub meter resolution (Darmawan, Walter, Richter, & Nikkoo, 2017). By using structure from motion technique (Szeliski, 2010), we are able to reconstruct high resolution Digital Elevation Model and orthomosaic of Anak Krakatau after the events.

The data were analyzed with high resolution Digital Elevation Model before the events and radar satellite image (sentinel 1A) post 22 December 2018 flank collapsed to track the topographic and structural changes due to the flank collapsed and the following eruptions.

Anak Krakatau is located in Sunda Strait (Figure. 1), where seismically active due to extensional and transition regimes of active oblique Sumatran and Java subductions (Harjono, Diament, Dubois, Larue, & Zen, 1991). It also lies on N20°E structure that delineated along Mt. Rajabasa, Sibesi, and Panaitan (Figure. 1). The extensional zone at Sunda Strait causing magma migration that accumulated at depth of 9 km and 22 km which is identified by strong seismic attenuation beneath Anak Krakatau (Abdurrachman, Widiyantoro, Priadi, & Ismail, 2018; Harjono, Diament, Nouaili, & Dubois, 1989; Jaxybulatov et al., 2011). Moreover, geochemistry analysis of the 2002 eruption samples suggests a plexus of smaller magma chambers that located at depth of 2 – 7 km, which is not clearly identified by seismic attenuation (Gardner et al., 2013). Continuous magma migration from the smaller chamber to the surface may interact with seawater and triggers surtseyan or phreatic or phreatomagmatic eruptions during its early reconstruction. The eruptions materials were deposited and reconstructed a volcanic cone (Fig. 2) that continuously deforms with growth range of 8 – 33 cm/month and progressively changes the morphology of Anak Krakatau (Sudrajat, 1982; SUTAWIDJAJA, 2006).

The morphology of Anak Krakatau is well documented since 1929 and regularly undergoes constructive and destructive phases (Zen, 1969) (Figure. 2). Constructive phase of Anak Krakatau was observed in 1929 until 1940's (~11 years), which then destroyed by series of eruptions between 1940's – 1950's. The eruptions continuously occurred between 1950's – 1960's, which followed by the deformation of a new cone at the crater lake and the expansion of the edifice of Anak Krakatau. Old topographic maps documented that the maximum elevation of Anak Krakatau edifice increased from 138.7 – 166.7 m above sea level (Decker & Hadikusumo, 1961). Series of eruptions between 1972 and 1973 destroyed some area at the south west of Anak Krakatau (Figure. 2). Afterward, the construction phase started again with intermittent eruptions and lava flows. The new cone that delineated by old crater rim was continuously deformed with maximum elevation increased from 180 m to ~315 m (Deplus et al., 1995; Hoffmann-Rothe et al., 2006).

2. The Methods

Generating Digital Elevation Model after the December flank collapsed and eruptions

We used a combination of drone photogrammetry and single beam echo sounder to reconstruct the high-resolution Digital Elevation Model of Anak Krakatau Volcano after the flank collapse on 22 December 2018. The field campaign was successfully realized during the summer period on 22-23

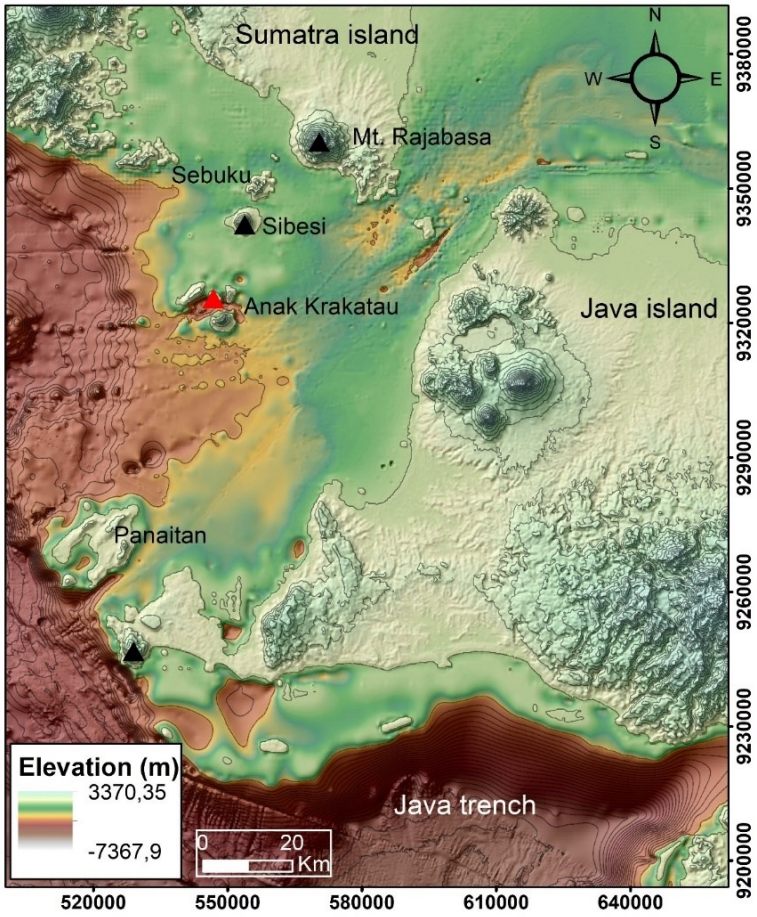

Figure 1. Topographic map of Anak Krakatau derived by Aster GDEM and Batnas shows the location of Anak Krakatau which lies on an extensional area between Sumatra and Java subductions zone and a N20°E structure from Mt. Rajabasa– Sebuku – Sibesi – Panaitan.

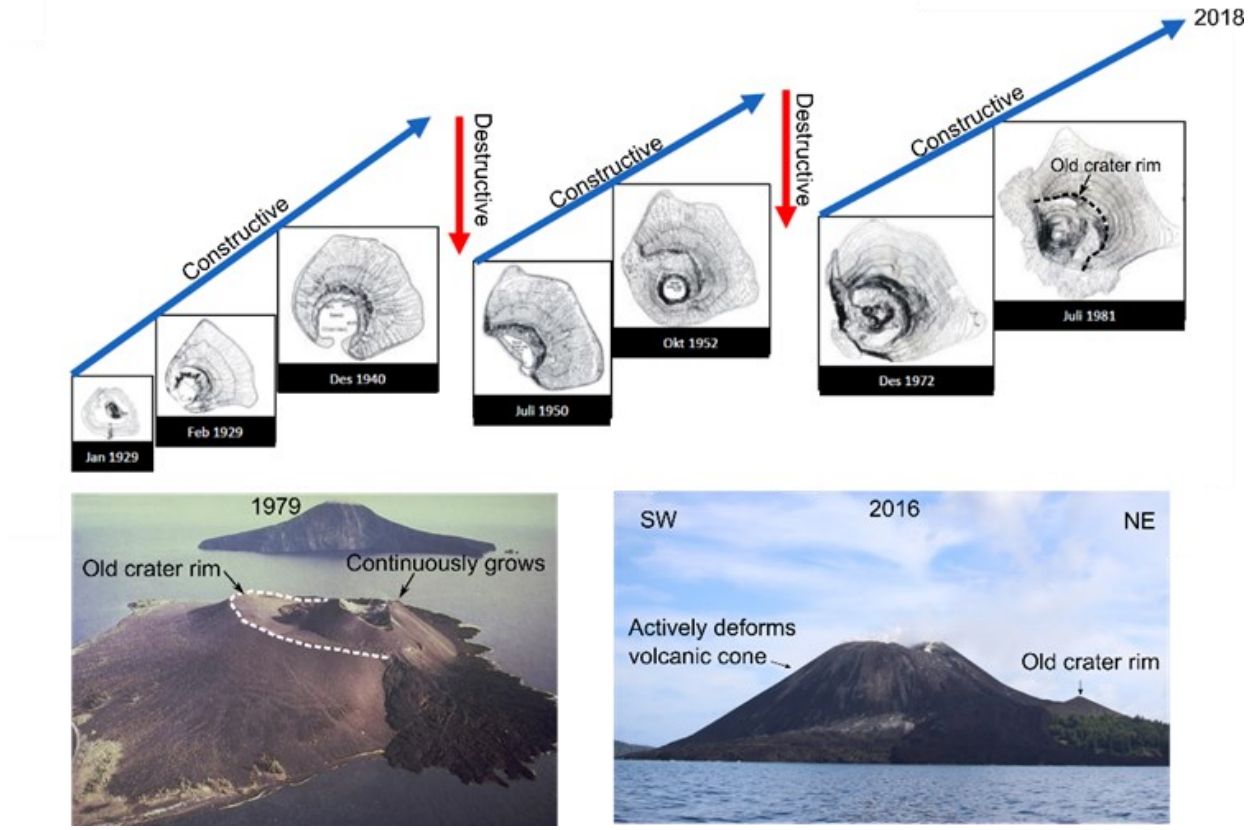

Figure 2. The morphology of Anak Krakatau is very dynamic. It was subjected to two times destructive phases before the December 2018 catastrophic events. The constructive phase mostly occurs at the active volcanic cone that continuously deforms and delineated by old crater rim as shown by the 1979 image from Volcanological Survey of Indonesia (VSI) and our 2016 photograph. Geomorphologically, the growth of active volcanic cone is close to the vicinity of steeply inclined crater wall that formed after the 1883 eruptions as shown by published bathymetry map (Deplus et al., 1995), which is prone to structural failure.

August 2019. For the drone photogrammetry, we used DJI Mavic pro attached with 12 megapixels camera. The drone flew at an altitude of ~300 – 350 m above the mean sea level (~150 m above Anak Krakatau), acquired images with nadir position for every 2 seconds. We obtained around 2627 overlap images that covered the edifice of Anak Krakatau volcano (Figure. 3). The images were processed by using Structure from Motion technique, which well implemented in Agisoft Metashape professional software to reconstruct a 3D model and a photomosaic image of the post-collapse of Anak Krakatau volcano.

We firstly checked the quality of the images and used only 2,610 images for data processing. Image alignment function was selected to generate a 3D sparse point cloud by setting the quality of "highest," pair selection of "reference," tie point limit of "40,000 points". These parameters used to obtain the highest quality of 3D sampled points based on feature and key points detection algorithm. The next step is building a 3D dense point cloud by set the quality of "moderate," depth filtering of "aggressive," and checked the calculate point colors. These settings allowed faster computational time with a high-quality result. Afterward, models of mesh, texture, and tile were built by setting the surface type of "height field", quality of "ultra-high," source data of "model," and blending mode of "mosaic." Ultra-high quality requires computational time, but an excellent and detail result during mesh generation. In the last step, we successfully generated high-resolution DEM and photomosaic of Anak Krakatau volcano by set the source data of "dense cloud" ant projection to "geographic UTM coordinate system." We then exported and merged the DEM with the DEM generated by the bathymetry technique to obtain topography of the post-collapse Anak Krakatau volcano.

A bathymetric data has extracted from the National Bathymetry of Indonesia at a scale of 6-arc-second. It produced by the Geospatial Information Agency of Indonesia (BIG) and was used to represent the pre-2018 CE bathymetry. Krakatau's post-2018 CE bathymetry was reconstructed using a GIS method based on the result of field measurements using a single-beam echo sounder. The advantage of this procedure is it allows further quantitative measurements such as volume difference (Mutaqin et al., 2019) between the pre and post-2018 CE eruption of Krakatoa volcano. In this study, we were able to interpolate data from field measurements to produce a post-2018 CE bathymetric model. The model is using the topo to raster method as it has been shown that it performs better than other methods on several different terrain types (Hutchinson, 1989). We then merged the high-resolution Digital Elevation Model and bathymetry to obtain topography model after the flank collapsed and the next following eruptions.

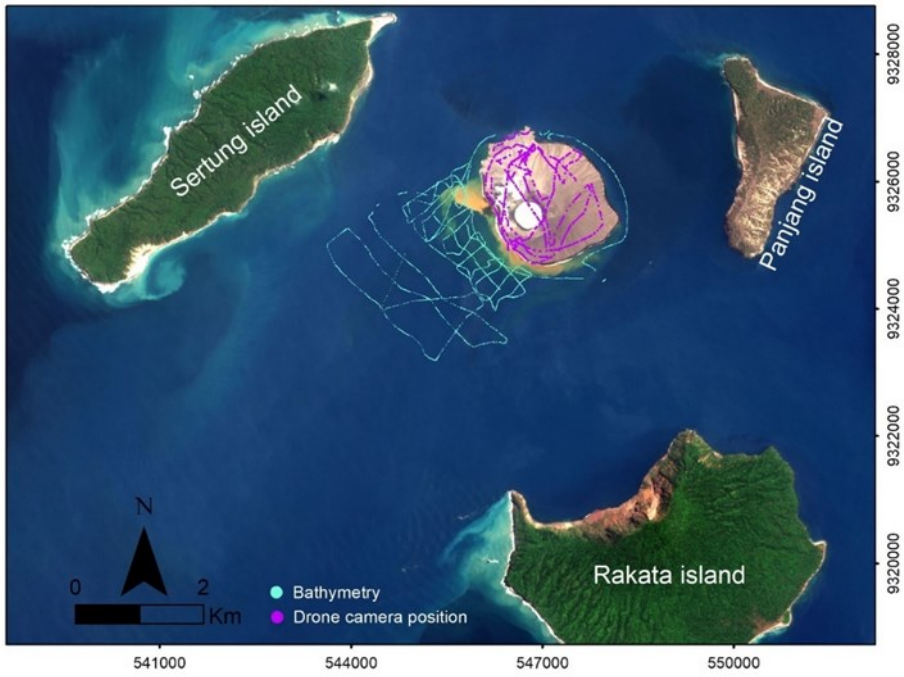

Figure 3. Distribution of sampled area to map the topographic of Anak Krakatau by using drone photogrammetry technique (purple dots) and single beam echo sounder (blue dots).

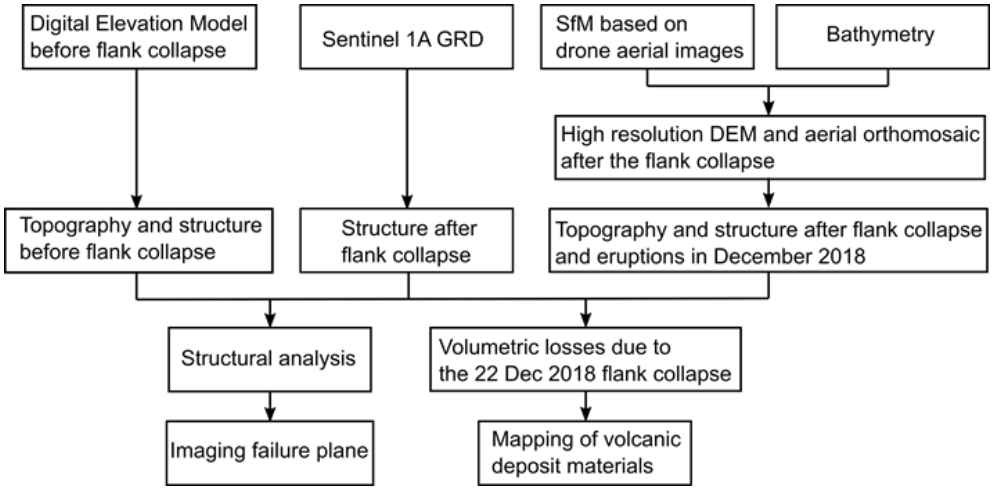

Figure 4. Flowchart of methodology

Topographic, structural changes and volumetric losses

We analyzed topographic and structural changes due to the flank collapsed and the eruptions by using high resolution DEM before , sentinel 1A GRD radar satellite images acquired on 22 December 2018 (shortly after flank collapsed), and our high-resolution drone photogrammetry DEM. High resolution before collapsed is available for free in DEMNAS (http://tides.big.go.id/DEMNAS/) with resolution of 8 m (Geospasial, 2018) and sentinel 1A GRD is available for free in sentinel hub download page (https://scihub.copernicus.eu/). Shortly after flank collapsed, high resolution satellite sentinel 1A with resolution of 10 m is able to track the structural changes due to 22 December 2018 flank collapsed at Anak Krakatau. Our DEM and orthomosaic derived by drone photogrammetry which has resolution of 1 m and 0,08 m can map more detail structure, altered area, blocks – bombs deposit, and volcanic sand materials at Anak Krakatau after the catastrophic events.

Moreover, we can track the volumetric losses due to the 22 December 2018 flank collapsed and the eruptions by using the structural changes to delineate the loss area for each event. We cropped the DEMs at the losses area before and after the 22 December 2018 flank collapsed and used cut and fill tools in ArcMap to calculate the volumetric losses. This tool is robust to quantify removal and additional area based on DEM pixel value. We performed similar technique to calculate the volumetric losses due to the next following eruptions (see figure 4 for the flowchart of methodology).

Mapping the distribution of volcanic materials

In order to map the distribution of volcanic materials due to flank collapsed and eruptions at Anak Krakatau, we firstly merged the DEMs of Anak Krakatau and bathymetry before the flank collapsed. We used again the cut and fill tool in ArcMap to map the distribution of volcanic materials. The losses area was then manually digitized in ArcMap to obtain the affected area. The losses area was overlaid over sentinel 2A satellite image for data visualization.

3. Results and Discussions

Topographic and structural changes

Before the 22 December flank collapsed, the morphology of Anak Krakatau was relatively steep at the volcanic cone with slope of >50° (Figure. 5a-a'). The active volcanic cone of Anak Krakatau was delineated by old crater rim with elevation of ~180 m and slope of 30°. At the lower flank, the surface roughness increased as it was possibly caused by the deposit of lava flows that occurred during reconstruction phase. The maximum diameter of the Anak Krakatau was 2,3 km from north to south. Structural mapping before the 22 December flank collapsed shows structures at the summit, at the west flank area, and at the old crater rim with length of ~300 m, 305 m, and 984 m, respectively.

Shortly after the 22 December 2018 flank collapsed, sentinel 1A captured the morphology of Anak Krakatau. As the dataset only contain amplitude (does not contain an information of elevation), we estimated the topography (Figure. 5b') based on the strong reflectance (white areas in figure 5b). We mapped around five structures that well correlate with the old crater rim, structures around conduit, and the west structure that already identified in the DEM before the events. The volume loss due to the 22 December flank collapsed is estimated ~127 x 10^6 m^3.

The next following eruptions after the 22 December 2018 flank collapsed caused changes of the morphology, topography and structures at Anak Krakatau (Figure. 5c-c'). The volume loss due to the eruptions is 0,8 x 10^6 m^3. The old crater rim now clearly visible with maximum length of ~2,6 km and delineated the loss area. We infer that the west and the old crater rim structures (red and blue bold lines in figure 5c) are the failure plane that may trigger the 22 December 2018 flank collapse of Anak Krakatau. The flank collapsed and the eruptions caused massive topographic loss from 305 m above sea level to 10 m below sea level. The current maximum diameter of Anak Krakatau is 2,1 km from north to south. The slope is mostly gently inclined with ~20°, except the crater wall that close to the crater pool where the slope is ~40°. The location of crater pool is also well correlated with the structures of conduit (black dash lines) (Figure. 5).

High resolution orthomosaic of drone images that has resolution of 8 cm can provide detail information of current morphology and surface deposit at Anak Krakatau (Figure. 6). During fieldwork in August 2019, most of the flank area has been eroded that causing streamlines. The eroded materials generate volcanic sand that abundantly found around the Anak Krakatau (Figure. 6b). Zoomed image of

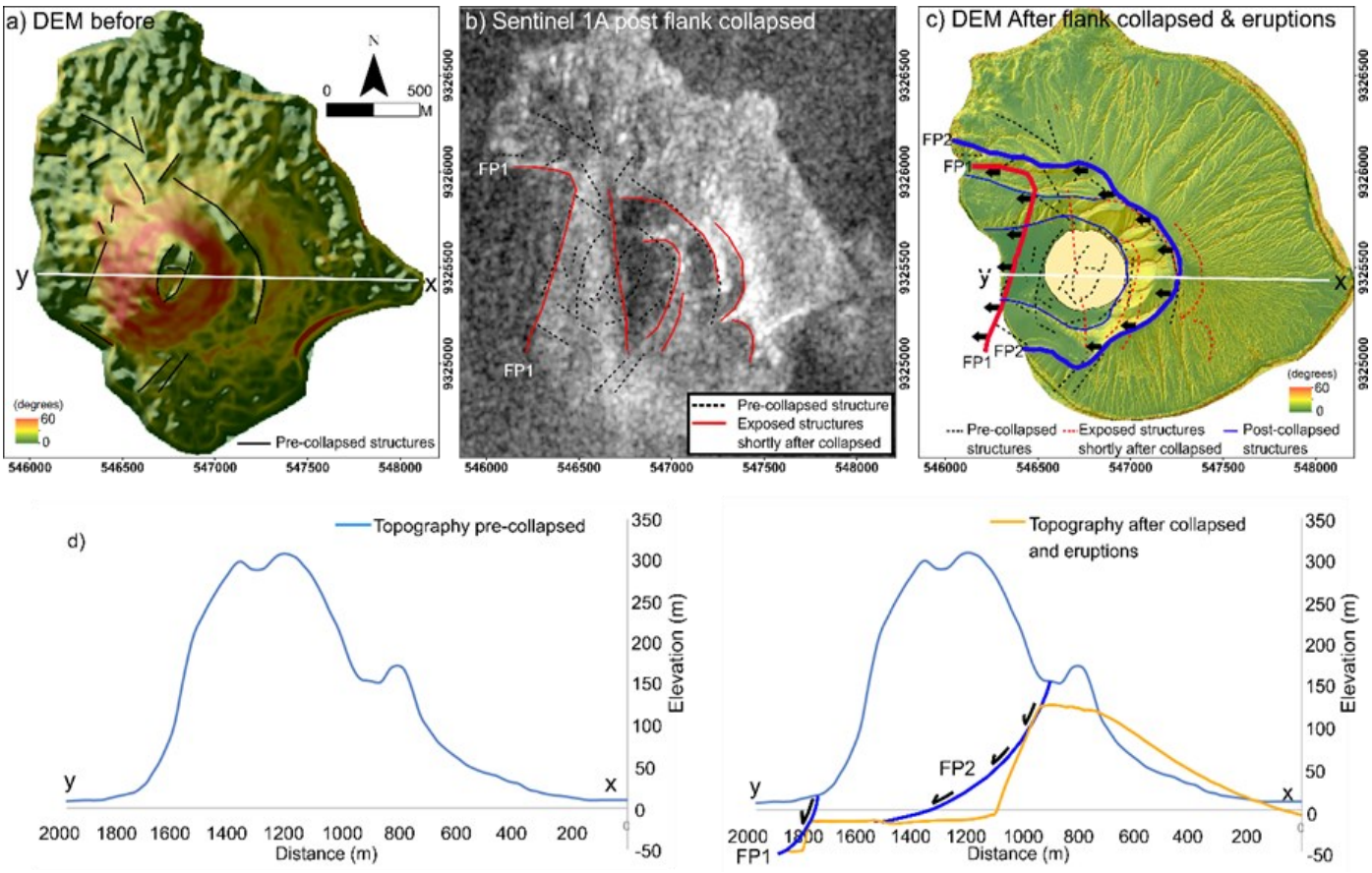

Figure 5. a) High resolution DEM before the December 2018 flank collapsed shows that the summit of Anak Krakatau was ~310 m, steeply inclined, delineated by old crater rim, had structures at the summit, and at the west part of the Anak Krakatau edifice. b) Shortly after the 22 December 2018 flank collapsed, some collapsed scar structures were exposed and highly correlated with the structures that already mapped before the collapsed event. c) High resolution DEM generated by drone photogrammetry can give more detail information of two main structures that possibly act as the failure plane (FP). d) The first failure plane (FP1) is the structure that located at the west part of the Anak Krakatau edifice (red line), while the second failure plane (FP2) is the old crater rim (blue line). The evidence of both failure plane is clearly observed in our orthomosaic image (Figure. 6)

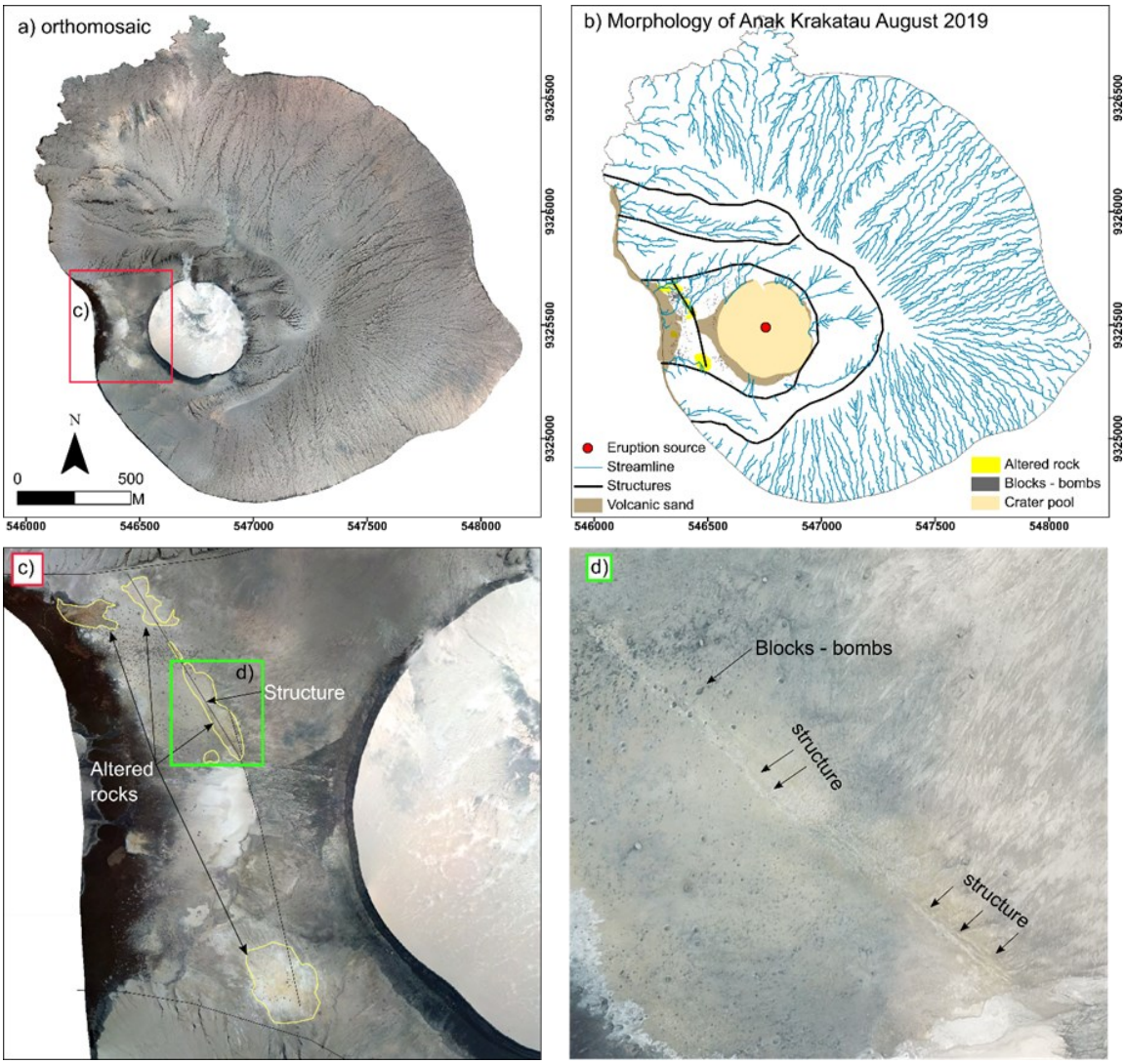

Figure 6. a) Our orthomosaic data that has resolution of 0,08 m clearly describes the morphology of Anak Krakatau after the December 2018 catastrophic events. b) Currently, a crater pool formed at the middle of the Anak Krakatau edifice and some eruptions intermittently occurs at the crater pool. The edifice of Anak Krakatau is covered by streamlines, which may indicate massive erosions. c and d) Zoomed image of the west part of Anak Krakatau can identify a structure that hydrothermally altered. The hydrothermal alteration can weaken the rock along the fracture which then may lead to failure

west area of crater pool clearly shows a structure that associated with hydrothermally altered rock (6c and d). Around the structure, we observed abundance of blocks – bombs with diameter of 0,01 – 5 m and loose materials in the west area.

Distribution of volcanic materials

The volcanic materials due to the 22 December 2018 flank collapsed and the following eruptions mostly distributed to the southwest area (red polygon in figure 7). The volcanic materials cover around 15 km² with maximum runout distance of 5,8 km from the current old crater rim. Before the catastrophic events, the maximum depth of the 1883 crater was 246 below sea level. Currently, the maximum depth becomes shallower to 215 m below sea level as the volcanic materials abundantly deposited at the southwest area, giving an average deposit thickness about 31 m.

Structural instability

One of the main factors that can trigger volcano flank collapsed is structural instability. In this study, our high-resolution DEM and orthomosaic clearly show the structural instability that might trigger the 22 December 2018 flank collapsed. We found two main failures plane that exposed after the December 2018 catastrophic events at Anak Krakatau (Figure. 5). The first failure plane is a structure that located at the west part of Anak Krakatau, close to the shore, and is associated with hydrothermal alteration. Hydrothermal alteration can reduce rock strength (Mordensky & Heap, 2019), internal friction (Meller & Kohl, 2014), and develop a weak core that can lead to structural weakening and flank collapse without large pore pressure (Cecchi, van Wyk de Vries, & Lavest, 2004; Darmawan, Walter, Troll, & Budi-santoso, 2018). In addition, other effect of hydrothermal alteration may trigger explosive behavior as the altered minerals seal the rock's porosity and lead to gas overpressure (Heap et al., 2019). The second failure plane is the old crater rim that delineated the actively deformed cone. This old crater rim is formed during constructive phase since 1920's and more stable, even though the edifice of Anak Krakatau was destroyed three times.

The structures that associated with hydrothermal alteration can cause the instability of Anak Krakatau edifice. Moreover, the eruptions activities and lava flows that

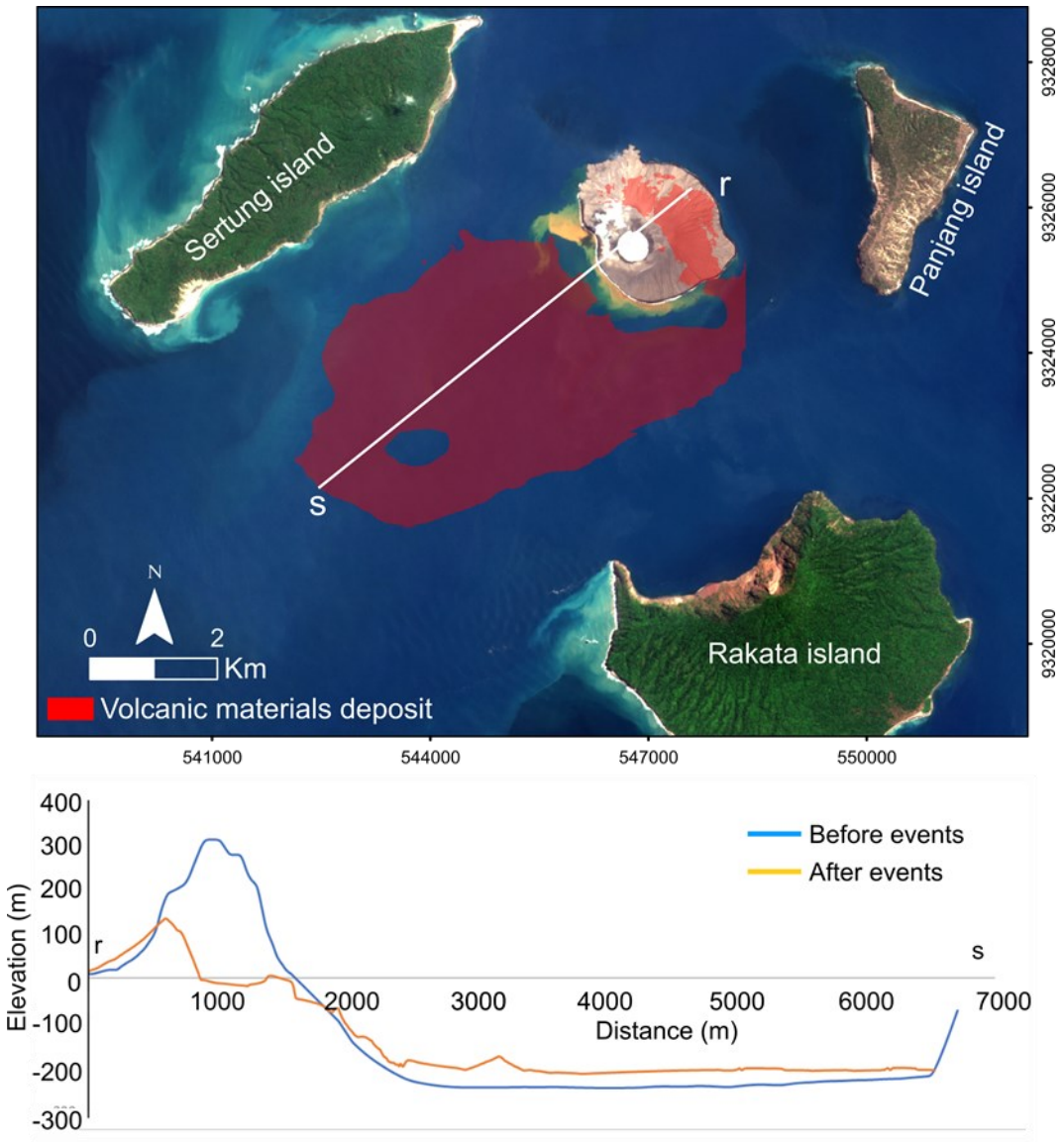

Figure 7. Cumulative distribution of volcanic materials due to the flank collapsed and the eruptions of Anak Krakatau in December 2018 (indicated by red polygon area) clearly shows that the deposit mostly covers the 1883 crater with mean thickness of ~31 m as shown by the cross section of line R-S. Based on the sentinel 2 image, it also suggests that the trees in Panjang island are burnt, possibly due to pyroclastic flows, unfortunately our bathymetry dataset is limited around Anak Krakatau volcanic island and south west area of Anak Krakatau (see Figure. 3). We infer that the volcanic materials are deposited at the sea floor between Anak Krakatau and Panjang island.

continuously occurred from January to December 2018 increased the land surface up to 3 km^2 (Walter et al., 2019) and may cause surface loading that flank oversteepening. As the actively deformed cone (see Figure. 2) was not stable structurally and geomorphologically, a small-high frequency earthquake that occurred 115 s prior to the event can trigger and lead to volcanic flank collapsed (Walter et al., 2019). Further seismic investigation suggested that the 22 December flank collapsed generated low frequency seismic with duration of 1 – 2 minutes and followed by a 5 min high frequency of strong gas emissions. This strong gas emissions possibly can generate high energetic pyroclastic flows that has runout distance of 5,8 km and burnt some trees in Panjang Island (Figure. 7).

Volumetric losses triggers tsunami in Sunda Strait

Our calculation suggests that the volume of the 22 December 2018 flank collapsed was 127 x 10^6 m^3. This number of volumes agrees with the estimation of volume flank collapsed based on the interpretation of Sentinel 1A datasets (Williams, Rowley, & Garthwaite, 2019), however, it is relatively lower compared with the volume used for numerical model of tsunami that was estimated to 0,23 km^3 (Grilli et al., 2019). We infer that 0.127 km^3 volume of flank collapsed could trigger tsunami in Sunda Strait with maximum height of 13 m along the coasts of Sumatra and west of Java (Muhari et al., 2019).

Current activities and future potential hazards

After the December 2018 catastrophic events that released high energy and pressure, the current activities of Anak Krakatau are dominated by low magnitude energy due to open conduit system. Nevertheless, surtseyan eruption commonly occurs as the eruption source is mostly located around sea level. These eruptions are dominantly phreatomagmatic eruptions, representing violent explosions

caused by rising basaltic or andesitic magma to the surface and contact with water. The ejected materials are mostly volcanic ash and ballistic projectile, which deposited around the crater.

Moreover, based on the historical activities since 1920's that well documented, Anak Krakatau is highly possible to reconstruct its edifice in the next futures. Effusive and explosive eruptions may occur intermittently, and the ejected volcanic materials are gradually deposited around the crater pool and progressively reconstructing the volcanic cone.

5. Conclusions

Our high-resolution drone datasets can show the evidence of structural instability that may contribute to the 22 December 2018 flank collapsed of Anak Krakatau. We conclude two structures that already weakened by hydrothermal activities beneath the Anak Krakatau edifice were destabilized by small magnitude of earthquake and acted as failure planes. The collapsed area was the area that actively deformed and delineated by old crater rim structure. Even though the collapsed volume was relatively small, however, it could generate devastating tsunami in Sunda Strait. In order to prevent similar volcanogenic tsunami event in the future, it is necessary to monitor the deformation of a new active volcanic cone of Anak Krakatau during reconstruction phase. We also recommend to identify the development of new structure at the edifice of Anak by using drone photogrammetry technique.

Acknowledgement

This study is funded by the Indonesian Ministry of Education and Research's program of INSINAS number 14/INS-2/PPK/E4/2019. We thank Nature Conservation Agency of Bengkulu Province for the permission, the boat and accommodation during fieldwork at Anak Krakatau Volcano. We also would like to thank Dr. Danang Sri Hadmoko for his generous suggestions and comments to improve the manuscript. Lastly, thanks to Dini Nuari Ardian, Agung Dwi Purnomo, and Pamungkas Yuliantoro for the field assistant.

References

Abdurrachman, M., Widiyantoro, S., Priadi, B., & Ismail, T. (2018). Geochemistry and structure of krakatoa volcano in the Sunda Strait, Indonesia. *Geosciences (Switzerland)*, *8*(4), 1–10. doi:10.3390/geosciences8040111

BNPB. (2019). Tsunami Selat Sunda.

Cecchi, E., van Wyk de Vries, B., & Lavest, J. M. (2004). Flank spreading and collapse of weak-cored volcanoes. *Bulletin of Volcanology*, *67*(1), 72–91. doi:10.1007/s00445-004-0369-3

Darmawan, H., Walter, T. R., Brotopuspito, K. S., Subandriyo, & Nandaka, I. G. M. A. (2018). Morphological and structural changes at the Merapi lava dome monitored in 2012–15 using unmanned aerial vehicles (UAVs). *Journal of Volcanology and Geothermal Research*, *349*, 256–267. doi:https://doi.org/10.1016/j.jvolgeores.2017.11.006

Darmawan, H., Walter, T.R., Richter, N., & Nikkoo, M. (2017). High resolution Digital Elevation Model of Merapi summit in 2015 generated by UAVs and TLS. GFZ Data Services. doi:http://doi.org/10.5880/GFZ.2.1.2017.003

Decker, R. W., & Hadikusumo, D. (1961). Results of the 1960 expedition to Krakatau. *Journal of Geophysical Research*, *66*(10), 3497–3511. doi:10.1029/jz066i010p03497

Deplus, C., Bonvalot, S., Dahrin, D., Diament, M., Harjono, H., & Dubois, J. (1995). Inner structure of the Krakatau volcanic complex (Indonesia) from gravity and bathymetry data. *Journal of Volcanology and Geothermal Research*, *64*(1–2), 23–52. doi:10.1016/0377-0273(94)00038-I

Famin, V., & Michon, L. (2010). Volcano destabilization by magma injections in a detachment. *Geology*, *38*(3), 219–222. doi:10.1130/G30717.1

Gardner, M. F., Troll, V. R., Gamble, J. A., Gertisser, R., Hart, G. L., Ellam, R. M., … Wolff, J. A. (2013). Crustal differentiation processes at Krakatau Volcano, Indonesia. *Journal of Petrology*, *54*(1), 150–182. doi:10.1093/petrology/egs066

Geospasial, B. I. (2018). DEMNAS. Retrieved from http://tides.big.go.id/DEMNAS/

Giachetti, T., Paris, R., Kelfoun, K., & Ontowirjo, B. (2012). Tsunami hazard related to a flank collapse of Anak Krakatau Volcano, Sunda Strait, Indonesia. *Geological Society Special Publication*, *361*(1), 79–90. doi:10.1144/SP361.7

Grilli, S. T., Tappin, D. R., Carey, S., Watt, S. F. L., Ward, S. N., Grilli, A. R., … Muin, M. (2019). Modelling of the tsunami from the December 22, 2018 lateral collapse of Anak Krakatau volcano in the Sunda Straits, Indonesia. *Scientific Reports*, *9*(1), 1–13. doi:10.1038/s41598-019-48327-6

Harjono, H., Diament, M., Dubois, J., Larue, M., & Zen, M. T. (1991). Seismicity of the Sunda Strait: Evidence for crustal extension and volcanological implications. *Tectonics*, *10*(1), 17–30. doi:10.1029/90TC00285

Harjono, H., Diament, M., Nouaili, L., & Dubois, J. (1989). Detection of magma bodies beneath Krakatau volcano (Indonesia) from anomalous shear waves. *Journal of Volcanology and Geothermal Research*, *39*(4), 335–348. doi:https://doi.org/10.1016/0377-0273(89)90097-8

Heap, M. J., Troll, V. R., Kushnir, A. R. L., Gilg, H. A., Collinson, A. S. D., Deegan, F. M., … Walter, T. R. (2019). Hydrothermal alteration of andesitic lava domes can lead to explosive volcanic behaviour. *Nature Communications*, *10*(1), 5063. doi:10.1038/s41467-019-13102-8

Hoffmann-Rothe, A., Ibs-von Seht, M., Knieß, R., Faber, E., Klinge, K., Reichert, C., … Patria, C. (2006). Monitoring Anak Krakatau Volcano in Indonesia. *Eos*, *87*(51). doi:10.1029/2006eo510002

Hutchinson, M. F. (1989). A new procedure for gridding elevation and stream line data with automatic removal of spurious pits. *Journal of Hydrology*, *106*(3), 211–232. doi:https://doi.org/10.1016/0022-1694(89)90073-5

Jaxybulatov, K., Koulakov, I., Seht, M. I., Klinge, K., Reichert, C., Dahren, B., & Troll, V. R. (2011). Evidence for high fluid/melt content beneath Krakatau volcano (Indonesia) from local earthquake tomography. *Journal of Volcanology and Geothermal Research*, *206*(3), 96–105. doi:https://doi.org/10.1016/j.jvolgeores.2011.06.009

Mayer, K., Scheu, B., Montanaro, C., Yilmaz, T. I., Isaia, R., Aßbichler, D., & Dingwell, D. B. (2016). Hydrothermal alteration of surficial rocks at Solfatara (Campi Flegrei): Petrophysical properties and implications for phreatic eruption processes. *Journal of Volcanology and Geothermal Research*, *320*, 128–143. doi:10.1016/j.jvolgeores.2016.04.020

Mcguire, W. J. (1996). Volcano instability: A review of contemporary themes. *Geological Society Special Publication*, *110*(110), 1–23. doi:10.1144/GSL.SP.1996.110.01.01

Meller, C., & Kohl, T. (2014). The significance of hydrothermal alteration zones for the mechanical behavior of a geothermal reservoir. *Geothermal Energy*, *2*(1), 1–21. doi:10.1186/s40517-014-0012-2

Mordensky, S. P., & Heap, M. J. (2019). Influence of alteration on the mechanical behaviour and failure mode of andesite: implications for shallow seismicity and volcano monitoring.

Muhari, A., Heidarzadeh, M., Susmoro, H., Nugroho, H. D., Kriswati, E., Supartoyo, … Arikawa, T. (2019). The December 2018 Anak Krakatau Volcano Tsunami as Inferred from Post-Tsunami Field Surveys and Spectral Analysis. *Pure and Applied Geophysics*, *176*(12), 5219–5233. doi:10.1007/

s00024-019-02358-2

Müller, D., Walter, T. R., Schöpa, A., Witt, T., Steinke, B., Gudmundsson, M. T., & Dürig, T. (2017). High-resolution digital elevation modeling from TLS and UAV campaign reveals structural complexity at the 2014/2015 Holuhraun Eruption site, Iceland. *Frontiers in Earth Science*, *5*(July), 1–15. doi:10.3389/feart.2017.00059

Mutaqin, B. W., Lavigne, F., Sudrajat, Y., Handayani, L., Lahitte, P., Virmoux, C., … Boillot-Airaksinen, K. (2019). Landscape evolution on the eastern part of Lombok (Indonesia) related to the 1257 CE eruption of the Samalas Volcano. *Geomorphology*, *327*, 338–350. doi:https://doi.org/10.1016/j.geomorph.2018.11.010

Sudrajat, A. (1982). The morphological development of Anak Krakatau volcano, Sunda Strait. *Geologi Indonesia*, *9*, 1–11.

Sutawidjaja, I. (2006). Pertumbuhan Gunung Api Anak Krakatau setelah letusan katastrofi s 1883. *Indonesian Journal on Geoscience*, *1*(3), 143–153. doi:10.17014/ijog.vol1no3.20063

Szeliski, R. (2010). *Computer Vision: Algorithms and Applications*.

USGS. (2017). 1980 Cataclysmic eruption. Retrieved from https://volcanoes.usgs.gov/volcanoes/st_helens/st_helens_geo_hist_99.html

Walter, T. R., Haghshenas Haghighi, M., Schneider, F. M., Coppola, D., Motagh, M., Saul, J., … Gaebler, P. (2019). Complex hazard cascade culminating in the Anak Krakatau sector collapse. *Nature Communications*, *10*(1). doi:10.1038/s41467-019-12284-5

Williams, R., Rowley, P., & Garthwaite, M. C. (2019). Reconstructing the Anak Krakatau flank collapse that caused the December 2018 Indonesian tsunami. *Geology*, *XX*(Xx), 1–4. doi:10.1130/g46517.1

Zen, M. T. (1969). The state of Anak Krakatau in September 1968. *Bulletin of National Institute of Geology and Mining*, *2*, 15–23.